Influence of boundary conditions on fluid dynamics in models of the cardiovascular system: a multiscale approach applied to the carotid bifurcation*

Rossella Balossino[1], Giancarlo Pennati[1], Francesco Migliavacca[1], Luca Formaggia[2], AlessandroVeneziani[2], Massimiliano Tuveri[2], Gabriele Dubini[1]

6th March 2006

1 Laboratory of Biological Structure Mechanics
Structural Engineering Department
Piazza Leonardo da Vinci, 32
20133 Milano, Italy

2 MOX– Modellistica e Calcolo Scientifico
Dipartimento di Matematica "F. Brioschi"
Politecnico di Milano
via Bonardi 9, 20133 Milano, Italy

Keywords: Multiscale model, hemodynamics, carotid artery bifurcation, stenosis.

Abstract

Background. This work aims at addressing an important problem in the simulation of detailed 3D hemodynamic models of vascular districts with complex anatomy. Namely, to define appropriate boundary conditions accounting for both local as well as global effects.

Method of Approach. The approach devised in this work is based on a multiscale model, where the Navier-Stokes equations for the district of interest are coupled to a non-linear system of ordinary differential equations which describes the global circulatory system as a lumped parameter network. The multiscale approach is applied to three 3D models of a carotid bifurcation which differ only in the severity of a stenosis in the internal carotid artery. The results of the multiscale simulations are compared to those obtained by two stand-alone models of the carotid bifurcation, which differ in the adopted strategy in prescribing the boundary conditions.

*This work has been supported by the EU Project "HaeModel"

Results. Significant differences are found in the results between the multiscale and the stand-alone models in terms of flows, pressures and wall shear stresses distribution in the 3D domain. Conclusions. The capability to numerically predict the hemodynamic changes due to the presence of a stenosis is highly dependent on the availability of correct boundary conditions. The geometrical multiscale approach offers a logical and proper alternative to the use of measured data to prescribe realistic boundary conditions and predict new hemodynamic scenarios.

1 Introduction

The circulatory system exhibits a multiscale nature due to the strong relationships between local and systemic phenomena in the circulation. An accurate analysis of the flow in a specific sub-region should take into account the fact that every district is part of a complex and interactive circulatory system. Local hemodynamics is responsible for pressure changes which in turn affect the blood flow distribution in downstream and upstream vessels or organs. Since a precise description in terms of morphology as well as fluid dynamics behaviour of the whole circulatory system is impossible, a promising solution is the use of a heterogeneous mathematical model, coupling a local and accurate model of the district of interest with a simplified model of the remaining vascular system [1, 2, 3, 4, 5, 6]. An example is here proposed to demonstrate the importance of applying proper boundary conditions when clinical data are not available or difficultly measurable. In particular, we consider a carotid artery bifurcation as an example to highlight the important contributions that correct computational fluid dynamics simulations may give in the quantitative evaluation of the hemodynamics. Computational studies [7, 8, 9, 10, 11, 12, 13] have emerged as potential tools to suggest possible explanations for pathologic phenomena reported in the literature regarding the study of atherogenesis and development of intimal hyperplasia in carotid arteries and its correlations with fluid dynamics. Nevertheless, since subtle changes in geometry can have a marked influence on the flow field and wall shear stress patterns, the true vascular geometry of specific patients, as well as individual flows and wall mechanical conditions are needed [12, 15]. Furthermore, computational fluid dynamics in arterial models coupled to theoretical models of intimal thickening or plaque formation was also suggested as a tool to predict future scenarios produced by a progressive disease [16, 17]. As concerns the boundary conditions, two main approaches were used in the literature to model the fluid dynamics in the carotid artery bifurcation: i) imposed inlet flow in the common carotid artery (CCA) and imposed flow at one of the outlets (internal carotid, ICA, or external carotid, ECA, arteries) and zero traction at the other outlet [7, 8, 9, 10, 11, 12, 13, 12, 15]; ii) imposed inlet flow in the CCA and zero traction (fixed pressures) at the outlets [19]. A different methodology is here proposed based on a multiscale approach: pressure boundary conditions obtained from a lumped parameter network of the circula-

tory system are applied at the boundaries of the 3D model. The hemodynamics of three realistic 3D models of a carotid bifurcation are investigated, which differ only in the degree of the stenosis in the ICA. Furthermore, the results from the multiscale simulations are compared to those obtained from stand-alone 3D models of the same stenosed carotid bifurcation, when two different approaches are used to prescribe the boundary conditions.

2 Materials and Methods

2.1 Mathematical models

We considered two different sub-models, a local one based on the 3D Navier-Stokes equations, and a global one based on a lumped-parameter representation. A finite volume method was adopted for the 3D model to solve the mass and momentum conservation equations derived for an incompressible Newtonian fluid:

$$\begin{cases} \rho\dfrac{\partial \mathbf{u}}{\partial t} + \rho\left(\mathbf{u}\cdot\nabla\right)\mathbf{u} - \mu\triangle\mathbf{u} + \nabla p = \mathbf{f} \\ \nabla\cdot\mathbf{u} = 0 \end{cases}, \tag{1}$$

where $\mathbf{u}, p$ are the blood velocity and pressure respectively, ρ is the density, μ the viscosity.

Three different geometries of a carotid bifurcation were considered. They differ only in the severity of a stenosis in the ICA. The 3D model without stenosis (model HEALTHY, Fig.1) was built using a data set obtained by high-resolution computed tomography (CT) scans of an autoptic specimen [20]. Imaging segmentation and automatic smoothing were operated by means of the AMIRA software (TGS Inc, San Diego, CA, USA). The reconstructed volume was then meshed with the Gambit software (Fluent Inc, Lebanon, NH, USA). A mesh with approximately 100,000 cells was adopted after a grid sensitivity analysis using unstructured grids. The stenosed models were built based on the same dataset of CT images except for a few images of the ICA that were manually modified to create a mild (model MILD) and a severe (model SEVERE) stenosis (Fig. 1). The minimum lumen areas created in the stenosed ICA are of 6.44 mm^2 and 1.89 mm^2, which correspond to a stenosis of about 65% and 90%, with respect to the model without stenosis, respectively. The inlet diameter of the CCA is 6.4 mm for all the models. A lumped-parameter model (LPM) provides a description of the whole circulatory system suitably split into its elementary districts or compartments, which are described by resistances (R), capacitances (C) and inductances (L). Blood flow and pressures in each compartment are linked by ordinary differential equations, which can be obtained by simplification of the Navier-Stokes model [21]. The following ordinary differential equations can be obtained from the momentum and mass conservation laws for the circulatory

districts:

$$Q_{in}(t) - Q_{out}(t) = C\frac{dP_{out}(t)}{dt}$$
$$P_{in}(t) - P_{out}(t) = RQ_{in}(t) + L\frac{dQ_{in}(t)}{dt} \tag{2}$$

where $Q_{in}(t), P_{in}(t)$ and $Q_{out}(t), P_{out}(t)$ indicate the instantaneous volumetric flow rate and pressure at the compartment inlet and outlet sections, respectively. The network is divided into several subsystems: the heart, the pulmonary circulation, the upper and lower systemic circulation (Fig. 1). The above equations are combined with the equations describing the heart model behavior. Time varying elastances are used to model both the ventricles and the atria; non linear resistances are adopted to describe the outflow and the inflow through the heart valves. More details about the equations describing the network can be found in [22]. The net parameter values are mostly derived from the literature [23]; some were adjusted in order to reproduce physiological CCA waveforms [Zohdi,Steinman] and flow division ratios between ICA and ECA (70% and 30% respectively) [25].

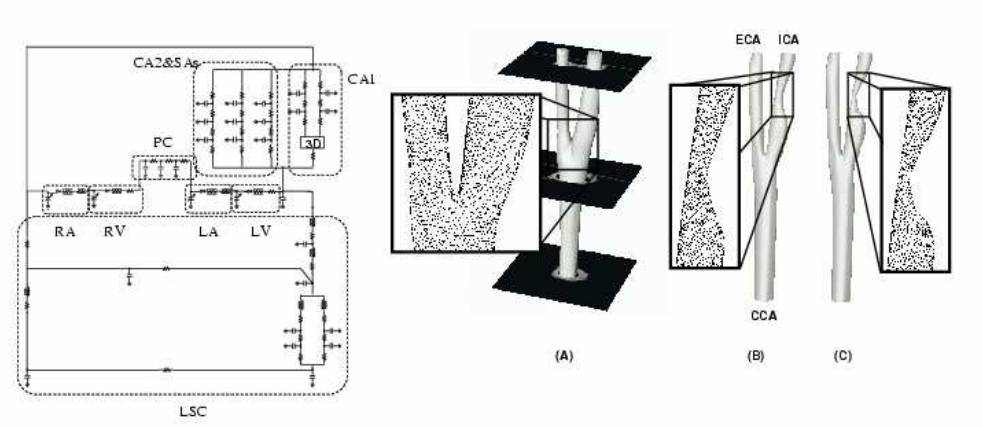

Figure 1: Lumped parameter model (left) of the circulatory system: CA1 carotid arteries connected to the 3D model; CA2,SAs the other carotid arteries and subclavian arteries; PC pulmonary circulation; LSC lower systemic circulation; RA, RV, LA and LV right atrium, right ventricle, left atrium and left ventricle, respectively. Representation of the three 3D models (right) used in the simulations: (A) healthy carotid bifurcation, (B) mildly stenosed carotid bifurcation (65%) and (C) severely stenosed carotid bifurcation (90%). Details of the meshes are reported, as well. CCA: common carotid artery; ECA: external carotid artery; ICA: internal carotid artery.

In general terms, the whole lumped parameter model is described by a nonlinear, differential-algebraic equation system in the form:

$$F(\dot{\mathbf{y}}(t), \mathbf{y}(t), t, \mathbf{b}) = 0 \tag{3}$$

where $\mathbf{y}(t)$ represents the unknown time-dependent vector and contains both flows and pressures ($Q(t)$ and $P(t)$ at each inlet and outlet compartment), t is the time and $\mathbf{b}$ is a vector containing forcing terms due to the interface conditions with the 3D model. This equation system is transformed into an ordinary differential equation (ODE) system after simple algebraic substitutions. The resulting ODE system is solved with an explicit Euler method, implemented in the Fluent code (Fluent Inc, Lebanon, NH, USA) by means of a user defined function. The coupling between the two sub-models is accomplished by means of the interface conditions: in particular pressures, calculated by the LPM, are the boundary conditions applied to the 3D model at the downstream and upstream sections. On the other hand the forcing terms in the ODE system depend on the interface volume flow rates calculated by the 3D model. In this way the local velocity profiles at the interfaces are not forced but calculated at each time step in a fully coupled manner. A detailed mathematical description of the multiscale methodology can be found in Quarteroni and Veneziani [3]. In the present paper, the interface boundary conditions are based on the prescription of pressures at the inlet and outlet boundaries of the carotid arteries. It is worth pointing out that it is also possible to simulate the multiscale circulation by imposing flow rate boundary conditions. Again, the velocity profiles are not prescribed, but they are computed by the numerical method [26].

2.2 Simulations.

Three different approaches were adopted in carrying out the simulations: a multiscale modeling applied to the three different geometries of the carotid bifurcation and two stand-alone models of the carotid bifurcation with different boundary condition. In the multiscale approach (MS) the boundary conditions, previously described, are exchanged between the two submodels in an iterative manner, avoiding any external prescription. The MS simulations were used for the three investigated 3D models. In the stand-alone modeling two simulations were carried out for each 3D model: i) Stand-Alone Pressure (SAP) simulation, where the pulsatile velocity profile obtained from the MS HEALTHY simulation is imposed at the inlet section of the 3D models, while constant and equal pressures are prescribed at the outlet sections [19]; ii) Stand-Alone Flow (SAF) simulation, where the pulsatile flow waveforms obtained from the MS HEALTHY simulation are imposed at the inlet and the ICA outlet section of the stenosed models assuming plug flow profiles; for this simulation a fixed pressure is set at the ECA outlet section [13, 14]. For all models the vessel walls are assumed rigid and no-slip conditions are imposed at the vessel walls; blood is treated as an incompressible, Newtonian fluid with a dynamic viscosity of 0.0035 $kg\ m^{-1}\ s^{-1}$ and a mass density of 1060 $kg\ m^{-3}$. The flow is assumed laminar [13]. Four cycles were simulated to ensure that flow is truly periodic, with a period of 0.8 seconds, corresponding to a heart rate of 75 beats per minute.

	Q_{CCA}	Q_{ICA}	Q_{ECA}	P_{ICA}	P_{ECA}
MS	6.61	4.71	1.90	1.60	1.01
SAP	**6.61**	3.97	2.64	1.18	1.18
SAF	**6.61**	**4.71**	1.90	1.60	1.01

Table 1: Results of the three boundary conditions approaches for the healthy case. Flow rates ([mm/l]), Pressures ([mmHg])

	Q_{CCA}	Q_{ICA}	Q_{ECA}	P_{ICA}	P_{ECA}
MS	6.56	4.65	1.91	3.23	0.97
SAP	**6.61**	2.91	3.70	1.73	1.73
SAF	**6.61**	**4.71**	1.90	2.92	0.82

Table 2: Results of the three boundary conditions approaches for the mildly occluded case. Flow rates ([mm/l]), Pressures ([mmHg])

3 Results and discussion

Results in terms of mean flow rates and pressure drops for the MS and stand-alone (SAP and SAF) models are summarized in Tab. 1, 2, 3.

First, we analyze the results obtained for the different MS models. A progressive, although slight, reduction of the mean total flow rate in the CCA of the MS models with increasing stenosis with respect to the HEALTHY model (6.61 and 6.56 vs. 6.05 ml/s) is detected. This reduction (-1.% and -8.5%, for MILD and SEVERE models, respectively) is due to the decrease in the ICA flow rate (-1.5% and -14.5%, for MILD and SEVERE models, respectively) which is only partially compensated by an increase in the ECA flow rate (+0.5% and +6%, for MILD and SEVERE models, respectively). The flow split between ICA and ECA branches remains almost unchanged even when the stenosis is severe (ICA flow percentage is 66.7% vs. 71.3% of the CCA flow rate in model SEVERE and HEALTHY, respectively), where a significant reduction could be expected in the internal branch because of the stenosis. Conversely, a severe stenosis produces a remarkable pressure gradient in the stenosed branch compared to the

	Q_{CCA}	Q_{ICA}	Q_{ECA}	P_{ICA}	P_{ECA}
MS	6.05	4.04	2.01	19.17	0.97
SAP	**6.61**	1.33	5.28	2.89	2.89
SAF	**6.61**	**4.71**	1.90	24.57	0.93

Table 3: Results of the three boundary conditions approaches for the severely occluded case. Flow rates ([mm/l]), Pressures ([mmHg])

HEALTHY model (19.17 mmHg vs 1.60 mmHg). The MS approach allows the evaluation of hemodynamics changes in the parts outside the 3D model. The presence of a mild or severe stenosis in the ICA reduces the flow entering the CCA (6.61 ml/s, 6.56 ml/s and 6.05 ml/s for the HEALTHY, MILD and SEVERE model, respectively) in favour of the flow directed to the other carotid and the subclavian arteries (5.35 ml/s, 5.38 ml/s and 5.67 ml/s for the HEALTHY, MILD and SEVERE model, respectively) and the descending aorta as calculated in the LPM. Furthermore, the observed results on flow repartition between ICA and ECA indicate that the resistances adopted in the LPM for the downstream districts representing the cerebral vascular bed are dominant if compared to the local resistance created by a 90% stenosis. Different values could be used for the cerebral parameters in the LPM in order to reproduce specific measured flow waveforms with different CCA flow as well as different ICA/ECA flow distribution. In any case, the MS approach would allow to predict how a physiological or pathological change in the 3D geometries can affect flow and pressures.

With respect to the stand-alone approaches different considerations may be done for the two methods. The SAP model gives markedly wrong results regardless the degree of the adopted stenosis, while the SAF model shows correct results for the mild stenosis and acceptable predictions when a 90% degree of stenosis is present.

The SAP approach causes a flow split between the two branches which directly depends on the resistance encountered by the blood flow throughout the sole 3D model, since the same pressure is imposed at the two outlets; the differences with the MS models are observed even in the HEALTHY case (ICA flow percentage is 60% vs. 71.3% of the CCA flow rate in SAP and MS models, respectively) and become huge for the stenosed models creating an unrealistic ECA flow dominance (ICA flow percentage is 44% and 20% of the CCA flow rate in SAP MILD and SAP SEVERE models, respectively). The discrepancies between the MS and SAP results are evident also in Fig. 2 where the velocity temporal tracings during a cardiac cycle at the inlet and outlet sections are reported for the investigated 3D models. Our findings indicate that the assumption of equal pressures at the two outlets [19] is rather erroneous when a stenosis occurs in one of the carotid branches (indeed, in the MS SEVERE simulation the ΔP_{ICA} is about 20 times higher than the ΔP_{ECA} as reported in Tab. 3). As concerns the SAF approach, the observed discrepancies with the MS method are a consequence of the boundary conditions imposed to the stenosed geometries which are derived from the MS HEALTHY simulation: indeed, the assumed ICA flow rate (4.71 ml/s) results only 17% higher than the MS one (4.04 ml/s), in the SAF SEVERE simulation leading to quite small errors also in the pressure drops. Actually, boundary volume flow rates are usually measured in vivo, together with the model geometry, since they are patient specific. When the flow rates in the CCA and the ICA or ECA may be directly measured by means of non-invasive techniques (e.g. ultrasound, MRI measurements [11, 12, 13, 14, 15]) use of measured flow rates as boundary conditions is surely the best choice for the

hemodynamic evaluation in specific patients. In particular, accurate calculation of quantities associated to the wall shear stress (for example, the time-average wall shear stress or the oscillatory shear index) are often performed since they are likely to be related to development and progression of arterial disease such as intimal thickening and atherosclerotic lesions. Several studies in the literature tried to predict the change in time of the vessel lumen due to the wall growth on the basis of the computed shear stress distribution [16, 17, 15]. However, in those works the adopted boundary conditions do not change with the evolution of the disease which progressively modifies the model geometry. Although important differences were not noted in the investigated constrictions, the simulations based on our multiscale approach showed that the carotid flow rates should be changed according to the increase in the lumen reduction due to presence of the stenosis. Figure 3 depicts the wall shear stresses magnitude at three different instants of the cardiac cycle for the model SEVERE as calculated according to the MS and SAF approaches. As expected, similar patterns occur for the two approaches, but with higher values of ICA wall shear stresses in the SAF approach. The two different shear stress distributions could lead to different conclusions about the progression of the disease. Thus, the prediction of hemodynamic changes due to the presence of a stenosis cannot be studied with a pure SAF approach since the model boundary conditions to be applied to future geometries are unknown. On the contrary a multiscale approach provides a logical and correct alternative for the imposition of realistic boundary conditions, since the investigated 3D geometries may be thought as three progressive stages of the arterial disease. In other words, the multiscale approach appears more realistic compared to the SAF one when new hemodynamics scenario are foreseen. Last, in the present study we considered the flow rates calculated by the MS HEALTHY as specific conditions for the reconstructed carotid geometry, since the actual flow rates were not available: in any case, we think that this limitation does not affect the general considerations of the study.

Conclusions

It has been showed that a stand alone 3D model with unrealistic boundary conditions at the sub-region interfaces could give misleading results, especially in the prediction of new hemodynamic scenarios. The multiscale approach has, instead, the advantage that the boundary conditions are not forced, but calculated and derived from the lumped model without any external imposition, that represents the remaining part of the circulatory system. However, our multiscale model still suffers from some limitations such as the assumption of rigid artery walls in the 3D model, the necessity of identification of the lumped parameter values for a specific patient, and the absence of any long-term mechanism of vascular adaptation.

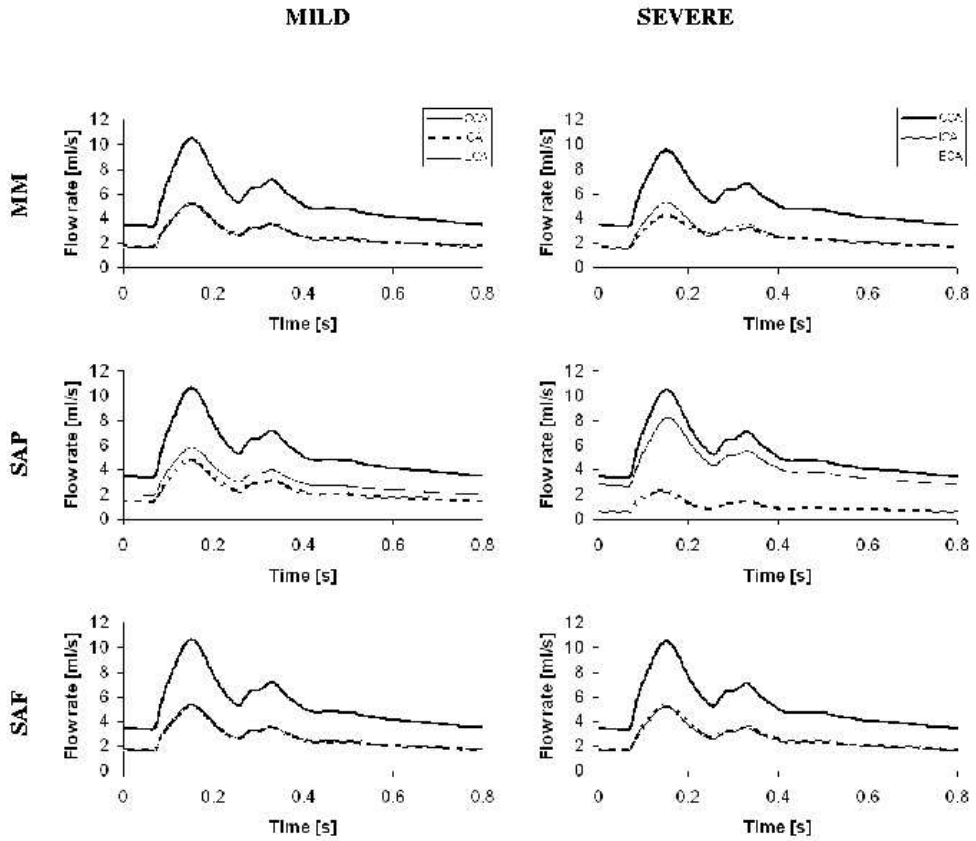

Figure 2: Flow rates during a cardiac cycle for the HEALTHY, MILD and SEVERE models: MS multiscale model; SAP stand alone pressure model with CCA flow rate equal to that in healthy case and fixed pressure at the outlets.

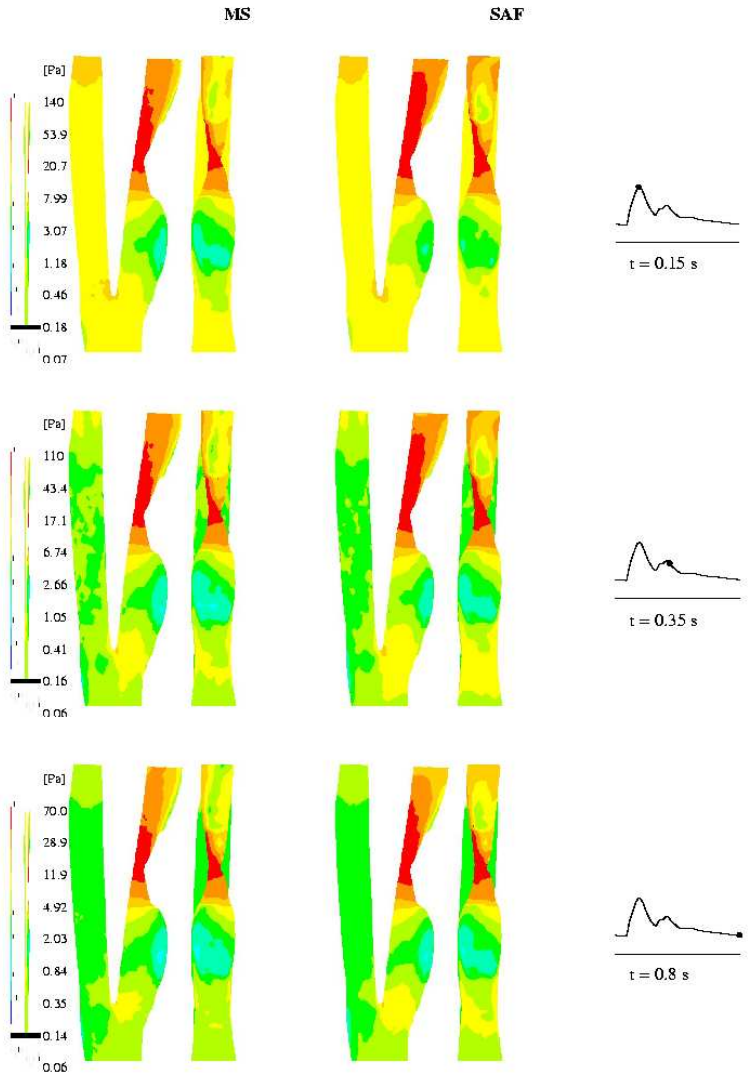

Figure 3: Two views of the contour maps of the wall shear stresses magnitude in three different instants of the cardiac cycle for the MS and the SAF of the SEVERE model. Scales are logarithmic and distinct for the various time instants in order to enhance the differences between the two approaches.

References

[1] Shim, E.B., Kamm, R.D., Heldt, T., and Mark, R.G., 2000, Numerical analysis of blood flow through a stenosed artery using a coupled, multiscale simulation method, Comput. Cardiol. 27, pp. 219-222.

[2] Laganà, K., Dubini, G., Migliavacca, F., Pietrabissa, R., Pennati, G., Veneziani, A., and Quarteroni, A., 2002, Multiscale modelling as a tool to prescribe realistic boundary conditions for the study of surgical procedures, Biorheology. 39, pp. 359-364.

[3] Quarteroni, A., and Veneziani, A., 2003, Analysis of a geometrical multiscale model based on the coupling of PDE's and ODE's for Blood Flow Simulations, SIAM J. on MMS., 1, pp. 173-195.

[4] Vignon, I., and Taylor, C.A., 2004, Outflow Boundary Conditions for One-dimensional Finite Element Modeling of Blood Flow and Pressure Waves in Arteries, Wave Motion, 39, pp. 361-374.

[5] Lagan, K., Balossino, R., Migliavacca, F., Pennati, G., Bove, E.L., de Leval, M.R., and Dubini, G., 2005, Multiscale modeling of the cardiovascular system: application to the study of pulmonary and coronary perfusions in the univentricular circulation, J. Biomech., 38, pp. 1129-1141.

[6] Formaggia, L. Nobile, F. Quarteroni, A., and Veneziani, A., 1999, Multiscale modeling of the circulatory system: a preliminary analysis, Computing and Visualisation in Science, 2, pp. 7583.

[7] Perktold, K., Resch, M., and Peter, R.O., 1991, Three-dimensional numerical analysis of pulsatile flow and wall shear stress in the carotid artery bifurcation, J. Biomech., 24, pp. 409-420.

[8] Perktold, K., and Rappitsch, G., 1995, Computer simulation of local blood flow and vessel mechanics in a compliant carotid artery bifurcation model, J. Biomech., 28, pp. 845-856.

[9] Long, Q., Xu, X.Y., Ariff, B., Thom, S.A., Hughes, A.D., and Stanton, A.V., 2000, Reconstruction of blood flow patterns in a human carotid bifurcation: a combined CFD and MRI study, J. Magn. Reson. Imaging, 11, pp. 299-311.

[10] Thomas, J.B., Milner, J.S., and Steinman, D.A., 2002, On the influence of vessel planarity on local hemodynamics at the human carotid bifurcation, Biorheology, 39(3-4), pp. 443-448.

[11] Papathanasopoulou, P., Zhao, S., Kohler, U., Robertson, M.B., Long, Q., Hoskins, P., Xu, X.Y., and Marshall, I., 2003, MRI measurement of time-resolved wall shear stress vectors in a carotid bifurcation model, and comparison with CFD predictions, J. Magn. Reson. Imaging, 17, pp. 153-162.

[12] Zhao, S.Z., Papathanasopoulou, P., Long, Q., Marshall, I., and Xu, X.Y., 2003, Comparative study of magnetic resonance imaging and image-based computational fluid dynamics for quantification of pulsatile flow in a carotid bifurcation phantom, Ann. Biomed. Eng., 31, pp. 962-971.

[13] Kaazempur-Mofrad, M.R., Isasi, A.G., Younis, H.F., Chan, R.C., Hinton, D.P., Sukhova, G., LaMuraglia, G.M., Lee, R.T., and Kamm, R.D., 2004, Characterization of the atherosclerotic carotid bifurcation using MRI, finite element modeling, and histology, Ann. Biomed, Eng., 32, pp. 932-946.

[14] Zhao, S.Z., Ariff, B., Long, Q., Hughes A.D., Thom, S.A., Stanton, A.V., and Xu, X.Y., 2002, Inter-individual variations in wall shear stress and mechanical stress distributions at the carotid artery bifurcation of healthy humans, J. Biomech., 35(10), pp. 1367-1377.

[15] Younis, H.F., Kaazempur-Mofrad, M.R., Chan, R.C., Isasi, A.G., Hinton, D.P., Chau, A.H., Kim, L.A., and Kamm, R.D., 2004, Hemodynamics and wall mechanics in human carotid bifurcation and its consequences for atherogenesis: investigation of inter-individual variation, Biomech. Model Mechanobiol., 3(1), pp. 17-32.

[16] Nazemi, M., Kleinstreuer, C., Archie, J.P., and Sorrell, F.Y., 1989, Fluid flow and plaque formation in an aortic bifurcation, J. Biomech. Eng., 111(4), pp. 316-324.

[17] Zohdi, T.I., 2005, A simple model for shear stress mediated lumen reduction in blood vessels, Biomech. Model. Mechanobiol., 4(1), pp. 57-61.

[18] Lee, D., and Chiu, J.J., 1996, Intimal thickening under shear in a carotid bifurcation–a numerical study, J. Biomech., 29(1), pp. 1-11.

[19] Stroud, J.S., Berger, S.A., and Saloner, D., 2002, Numerical analysis of flow through a severely stenotic carotid artery bifurcation, ASME J. Biomech. Eng., 124, pp. 9-20.

[20] Abdoulaev, G., Cadeddu, S., Delussu, G., Donzelli, M., Formaggia, L., Giochetti, A., Gobbetti, E., Leone, A., Manzi, C., Pili, P., Scheinine, A., Tuveri, M., Varone, A., Veneziani, A., Zanetti, G., and Zorcolo, A., 1998, ViVa: the virtual vascular project, IEEE Trans. Inf. Technol. Biomed., 2(4), pp. 268-274.

[21] Quarteroni, A., Ragni S., and Veneziani, A., 2001, Coupling between lumped and distributed models for blood flow problems , Computing and Visualization in Science, 4(2), pp.111-124.

[22] Migliavacca, F., Pennati, G., Dubini, G., Fumero, R., Pietrabissa, R., Urcelay, G., Bove, E.L., Hsia, T.Y., de Leval, M.R., 2001, Modeling of the Norwood circulation: effects of shunt size, vascular resistances, and heart rate, Am. J. Physiol. Heart Circ. Physiol., 280, pp. H2076-H2086.

[23] Rideout, V.C., 1972, Cardiovascular system simulation in biomedical engineering education, IEEE Trans. Biomed. Eng., 19, pp. 101-117.

[24] Steinman, D.A., Thomas, J.B., Ladak, H.M., Milner, J.S., Rutt, B.K. and Spence, J.D., 2002, Reconstruction of carotid bifurcation hemodynamics and wall thickness using computational fluid dynamics and MRI, Magnetic Resonance in Medicine, 47, pp. 149-159.

[25] Marshall, I., Papathanasopoulou, P., Wartolowska, K., 2004, Carotid flow rates and flow division at the bifurcation in healthy volunteers, Physiol Meas., 25(3), pp. 691-697.

[26] Veneziani, A., and Vergara, C., 2005, Flow rate defective boundary conditions in haemodynamics, Int. J. Num. Meth. Fluids, 47, pp. 803-816.